ELSEVIER

Polymer 43 (2002) 503–507

polymer

www.elsevier.com/locate/polymer

Time evolution of dynamic heterogeneity in a polymeric glass: a molecular dynamics simulation study ☆

Wenzheng Jin, Richard H. Boyd*

Department of Materials Science and Engineering, University of Utah, Room 304, 122 S. Central Campus Drive, Salt Lake City, UT 84112-0560, USA

Abstract

Dynamic heterogeneity, where it is noticed in molecular dynamics (MD) simulations that, for example, conformational transition rates vary greatly from bond to bond, is characteristic of polymeric glasses. The phenomenon can be attributed to the fact that certain local bond sequences are more capable of conformational rearrangement than others. These local sequences become fixed sites when the overall chain trajectory is frozen-in in the glass. Although this is no doubt the case, because of the relatively short times of MD trajectories and the relatively small numbers of transitions it is important to establish that the heterogeneity does evolve in time in the manner expected from the local site picture and is not an artifact of short simulations or small numbers. This is undertaken here using a polyethylene system that has been much studied previously. Long trajectories are generated where the time evolution of heterogeneity can be studied. It is found that both the standard deviation and the mean value of the transitions over the bonds evolve linearly in time. This is consistent with the local fixed site picture and not with a random process involving relatively small numbers of transitions.

Keywords: Vitrification; Dynamic heterogeneity; Molecular dynamics simulation

1. Introduction

The vitrification of melts upon cooling is one of the most interesting and practically important aspects of polymeric materials behavior. Especially intriguing is the fact that most polymers retain motional processes in the glass even though the cooperative segmental chain rearrangements characteristic of the melt have been frozen out. These processes are manifested as 'subglass' relaxations that can be well characterized by various experimental techniques such as mechanical, dielectric and NMR spectroscopy [1,2]. The question of how polymer molecules manage to undergo rearrangement in a rigid glass where the cooperative segmental rearrangements no longer take place is a longstanding one [3]. One of the clues is that the subglass motions apparently involve a length scale considerably shorter the segmental motions in the melt. Also implied then is that the motions are localized spatially and do not interact to the extent of resulting in the cooperativity found in the melt. That is, they take place at certain favorable places in the chain that have a long-term identity. The extreme relaxation breadth found in time or frequency domain measurements is to be attributed to the several kinds of favorable conformations available and to the vagaries of the packing, which also contributes substantially to the activation energetics at given sites. Historically there have been many suggestions as to the detailed nature of the molecular rearrangements involved. Crankshaft motions proposed as underlying the γ relaxation in polyethylene (PE) were the perhaps most famous [4,5]. In summary, the glass is viewed as dynamically heterogeneous where molecular rearrangements do take place but at certain favored locations.

The advent of long trajectory molecular dynamics (MD) simulations (currently approaching a microsecond) on bulk polymer melts and glasses has made the detailed examination of the above questions possible. In PE, in solution [6,7] and in bulk [8–10], it is now known that several types of next-neighbor correlated conformational jumps that leave the overall chain trajectory relatively undisturbed are involved. In addition, self-correlated over and back motions of one bond take place in local environments where a barrier traverse can be made from average positions that are displaced somewhat towards the barrier from the minimum in the torsional potential [10,19]. In other polymers, such as polybutadienes for example [11,12], local conformational transitions take place that are characteristic of the chain structure. The general result is that conformational transitions are found to take place highly preferentially at certain

☆ This paper was originally submitted to *Computational and Theoretical Polymer Science* and received on 22 November 2000; received in revised form on 9 February 2001; accepted on 9 February 2001. Following the incorporation of *Computational and Theoretical Polymer Science* into *Polymer*, this paper was consequently accepted for publication in *Polymer*.

* Corresponding author. Tel.: +1-801-581-6865; fax: +1-801-581-4816.
E-mail address: boyd@poly2.mse.utah.edu (R.H. Boyd).

0032-3861/02/$ - see front matter
PII: S0032-3861(01)00419-0

bonds and certain local sequences of bonds. Dynamic heterogeneity prevails. In contrast, in the melt over the time scale of a simulation where complete relaxation occurs (i.e. complete autocorrelation function decay of a monitored property) all of the bonds are equivalent with respect to conformational transitions. It is presumed then that the appearance and disappearance of this heterogeneity on cooling and heating is an important descriptor of the vitrification process.

The purpose of the present work is to demonstrate that the dynamic heterogeneity found in the glass in simulation is indeed stable over time scales characteristic of the characterizing experiments and not an artefact or transient effect associated with short MD trajectories. To accomplish this we examine the evolution of the heterogeneity over time in a long MD trajectory in PE glass and compare its behavior with that to be expected on the basis of distributed fixed local sites in the glass that have differing rates of conformational transitions.

2. Simulation details

The PE system utilized is one we have used in a number of studies [9,10,13,14]. Since trajectory length is of prime importance in relaxation studies it is crucial that computational speed be as high as possible consistent with physical realism. Thus the CH_2 representation is of the united atom type but with the force center displaced to give more realistic anisotropy to the packing (anisotropic united atom, AUA representation) [15]. The force field or energy parameters are repeated here in Table 1. The periodic box size is 768 CH_2 units, but in contrast to our previous work it consists of four equal length chains rather than a single one. The non-bonded cut-off radius was 9 Å but continuum corrections to the energy and force are made beyond this distance [16].

The system was prepared from an existing single chain system by deleting the appropriate bonds and equilibration at 500 K. The system was cooled under NPT (particle number, pressure, temperature) dynamics to desired temperatures and equilibrated isothermally. The isothermal runs were made under NVT (volume) dynamics [17] and in order to further enhance computational speed a multi-time step explicit reversible integrator method was used [18,19]. The inner loop that excludes the non-bonded forces has a time step of 1 fs and for the complete outer loop it is 5 fs. This partition was established in preliminary work where stability of energy conservation in NVE dynamics was monitored and in comparisons of NVT trajectories with and without the multiple time steps. The volume–temperature results were in good agreement with those previously obtained for the single chain system [9,10], the extra chain ends and any effect on packing not being noticeable at the resolution of the simulations. The single chain system gives V–T results [13] in agreement with experiment at higher temperatures where data is available for amorphous PE.

In enumerating conformational transitions the definition is used that the torsional angle must proceed from within $\pm 10^\circ$ of a minimum in the torsional potential to within $\pm 10^\circ$ of another minimum for a transition to have occurred.

Trajectories were generated at four temperatures in the glass, 150, 180, 200 and 220 K. The highest temperature corresponds approximately to the volumetric glass transition found in MD generated volume vs. temperature curves at constant pressure [9,10]. At the three highest temperatures, the total trajectories were 250 ns and at 150 K, the trajectory was extended to 400 ns to order to give more transitions. The total number and distribution of transitions as accumulated at 50 ns intervals are used to describe the time evolution. The initial 50 ns intervals contained slightly more transitions than the ensuing ones, an effect observed as a noticeable positive intercept in plots of accumulated transitions versus time. Although the systems were equilibrated for several ns before data accumulation this is probably due to some further equilibration at the start of the long trajectories. In any event, this observation doe not have an effect on the conclusions drawn.

3. Results and discussion

3.1. Conformational transitions. Localized sites vs. random occurrence

A convenient way, and one used by us in previous studies, to summarize dynamic heterogeneity is to record the number of conformational transitions over a fixed time period for each bond [9]. Fig. 1 shows typical results in terms of a 'spike' plot. The transitions are plotted against bond number as enumerated serially along each chain in

Table 1
Potential functions (energies in kJ/mol, distances in Å, angles in radians (shown above in degrees), the potentials are from Ref. [13])

Function	Constants	
C–C bond stretch energy $= (1/2)k_R(R - R_0)^2$	$k_R = 663$	$R_0 = 1.54$
Bond bending energy $= (1/2)k_\theta(\theta - \theta_0)^2$, $-CH_2-$ (PE)	$k_\theta = 482$	$\theta_0 = 111.6^\circ$
Torsional potential $= (1/2)V_3(1 + \cos 3\phi) + (1/2)V_1(1 + \cos \phi)$	$V_3 = 13.4$	$V_1 = 3.35$
AUA nonbonded potential, Lennard–Jones 6–12[a], $-CH_2-$	$\varepsilon = 0.686$	$R_{min} = 3.940$; $\sigma = 3.510$; $d = 0.42$

[a] For the $-CH_2-$ group, the potential is of the 'AUA' (anisotropic united atom) type, the interaction center is offset from the C atom by the distance $= d$ along the bisector of the C–C–C angle in the direction of the hydrogens; ε is the well-depth; R_{min} is the distance at the minimum; σ is the corresponding distance at the energy zero.

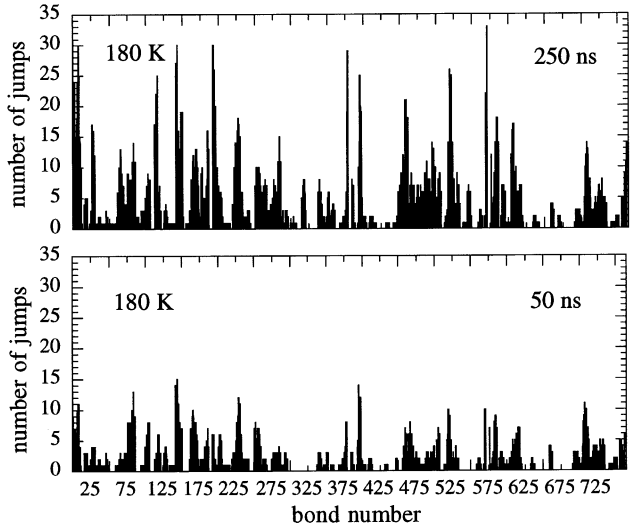

Fig. 1. The number of transitions at each bond vs. the bond location, 180 K. The lower panel is the accumulated number after 50 ns and the upper one after 250 ns.

sequence. The two panels in Fig. 1 show the distribution of transitions after 50 and 250 ns. The number of transitions has increased at the longer time but it would also appear that the obvious heterogeneity in transitions is maintained.

A statistical measure of the dispersion in the numbers of transitions per bond over the all bonds can be computed. Because the number of transitions per bond can be small over a trajectory, even for a random distribution, and therefore not a dynamically heterogeneous one, the dispersion need not be zero. For a random, or Poisson distribution of transitions per bond, the standard deviation, σ_P, is $X^{1/2}$ where X is the average number of transitions per bond [20,21]. As a measure of non-randomness or heterogeneity the comparison of the actual standard deviation found in simulation, σ with the Poisson value is diagnostic. Values of σ greater than σ_P indicate inherent heterogeneity.

It is appropriate here to describe the expected time evolution behavior of the heterogeneity under the situation where conformational transitions take place at different rates at different independent localized sites. The sites are presumed to be identified with different local conformational sequences that are fixed spatially because the overall chain trajectory is fixed by being in a glass. Thus for a site, i, the rate of conformational transitions or jumps, can be considered to be described by a rate constant, k_i, and therefore the jumps, N_i, at i evolve as

$$N_i = k_i t \tag{1}$$

and

$$X = \sum_{i=1}^{N_B} N_i/N_B = \langle k_i \rangle t, \tag{2}$$

where the $\langle\ \rangle$ brackets indicate the averaging over sites (bonds, of N_B total number). It might be that at many bonds the rate constants are very small and no transitions are observed or that the number of transitions at a given bond in an MD trajectory are so small as to not give rise reliably to an observed linear rate. However in a trajectory long enough that the total number of transitions is considerable it is to be expected, and in fact is observed, that the average number of transitions per bond, X, will be linear in time. The standard deviation of the number of transitions, N_i, about the average X, is

$$\sigma = \left(\sum_{i=1}^{N_B} (N_i - X)^2/N_B\right)^{1/2} = \left(\left(\sum_{i=1}^{N_B} N_i^2/N_B\right) - X^2\right)^{1/2}, \tag{3}$$

$$\sigma = t(\langle k_i^2 \rangle - \langle k_i \rangle^2)^{1/2}. \tag{4}$$

Thus the standard deviation evolves linearly in time. In contrast, the random or Poisson value ($\sigma_P = X^{1/2}$) evolves as the square root of time. Therefore there is a clear and convenient distinction between the two cases.

3.2. Heterogeneity of conformational transitions vs. time: observed behavior

As indicated above, the transitions increase linearly in time. More importantly in the present context the standard deviation of the spatial distribution should also increase linearly in time for the case of a fixed heterogeneous distribution of sites. But if in the longer term there were a trend towards homogenization, the standard deviation should drift towards the lower values of σ and square-root time dependence characteristic of a random distribution. Figs. 2–5 examine this issue at the four temperatures studied. The number of transitions per bond, X, as enumerated in simulation and the observed standard deviation of the transitions over the bonds, σ are plotted vs. time. It is apparent,

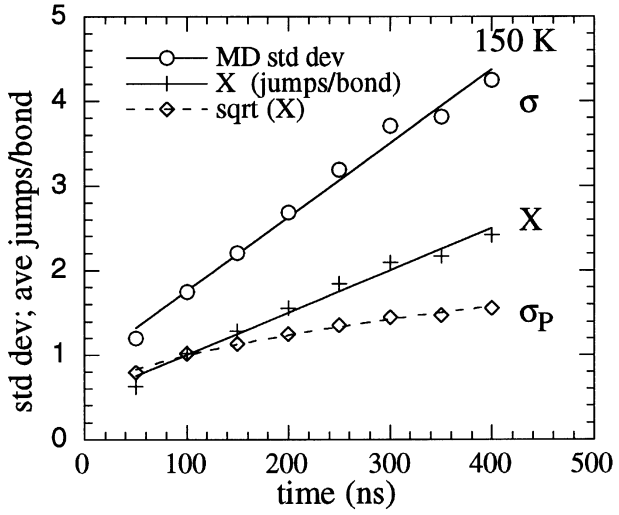

Fig. 2. The standard deviation of the accumulated transitions, σ, and the average number of transitions per bond, X, vs. time as found in MD simulation at 150 K. Also shown is the standard deviation of the transitions, $\sigma_P = X^{1/2}$, that would have resulted if the distribution were random (Poisson distribution). The curves through σ and X are linear regressions. The dashed curve through σ_P is a regression of the function $a + bt^{1/2}$.

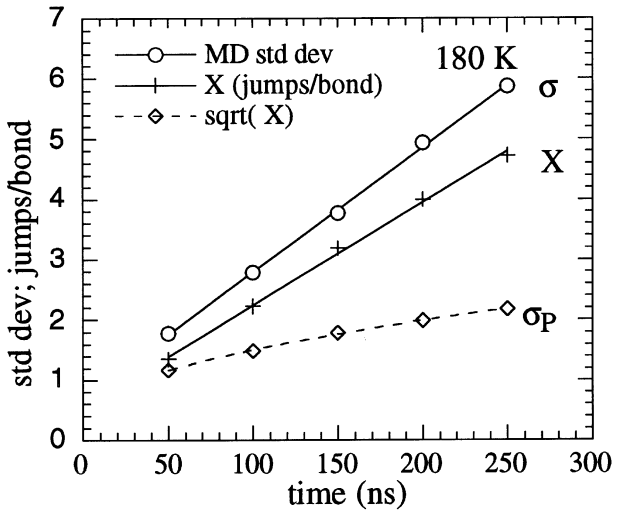

Fig. 3. The standard deviation of the accumulated transitions, σ, and the average number of transitions per bond, X, vs. time at 180 K; see Fig. 2 for details.

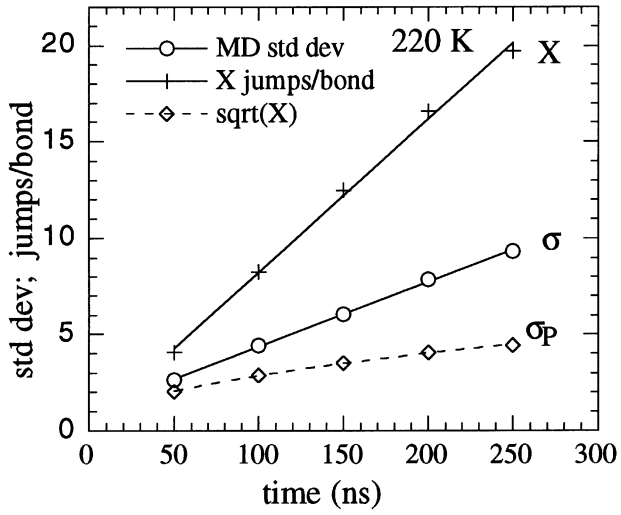

Fig. 5. The standard deviation of the accumulated transitions, σ, and the average number of transitions per bond, X, vs. time at 220 K; see Fig. 2 for details.

even though some scatter is found at 150 K, both X and σ evolve linearly in time. Also shown is the standard deviation that would have resulted from the observed number of transitions per bond, X, if the distribution were random, i.e. $\sigma_P = X^{1/2}$. It is evident that this measure is far smaller than the observed standard deviation and follows a different time evolution than that actually observed for the standard deviation. Thus the time evolutions are entirely consistent with the concept of a distribution of fixed independent sites.

3.3. Heterogeneity of conformational transitions: effect of temperature

It may be seen in Figs. 2–5 that as temperature increases the value of σ relative to X decreases. The result itself can be attributed to the effect of temperature on the rates at the individual sites. Suppose the rate constants, k_i are Arrhenius in nature and vary from site to site due to variations in activation energies, E_i^*, (but not front factors, A) or

$$k_i = A\, e^{-E_i^*/RT}. \tag{5}$$

Further, suppose the distribution of site activation energies is continuous and represented by a normalized distribution, $P(E^*)$. Then $\langle k_i\rangle$ and $\langle k_i^2\rangle$ in Eqs. (2) and (4) become

$$\langle k_i\rangle = A\int P(E^*)\, e^{-E_i^*/RT}\, dE^*, \tag{6a}$$

$$\langle k_i^2\rangle = A^2\int P(E^*)\, e^{-2E_i^*/RT}\, dE^*. \tag{6b}$$

For purposes of illustration, a Gaussian distribution about a central activation energy, E_0^*, may be utilized

$$P(E^*) = 2\sqrt{b/\pi}\, e^{-b(E^*-E_0^*)^2}, \tag{7}$$

where the mean square dispersion about E_0^* is $\langle(E^* - E_0^*)^2\rangle$ is given by $1/(2b)$. Use of the Gaussian distribution in Eqs. (6a) and (6b) leads to

$$\langle k_i >= k_0\, e^{1/[4b(RT)^2]}; \qquad k_0 = A\, e^{-E_0^*/RT}, \tag{8a}$$

$$\langle k_i^2\rangle = k_0^2\, e^{1/[b(RT)^2]}. \tag{8b}$$

The ratio of σ to X in question then is given by

$$\sigma/X = (\langle k_i^2\rangle/\langle k_i\rangle^2 - 1)^{1/2} = (e^u - 1)^{1/2};$$
$$u = \langle(E^* - E_0^*)^2\rangle/(RT)^2 \tag{9}$$

It is apparent from Eq. (9) that the ratio σ/X must

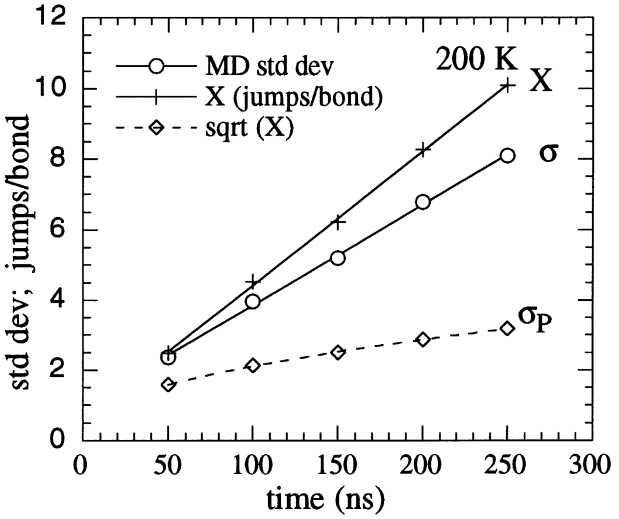

Fig. 4. The standard deviation of the accumulated transitions, σ, and the average number of transitions per bond, X, vs. time at 200 K; see Fig. 2 for details.

Table 2
Temperature dependence of heterogeneity

T (K)	σ/X, MD simulation[a]	σ/X, calcd Eq. (9)[b]
150	1.75	1.61
180	1.21	1.21
200	0.75	1.03
220	0.42	0.90

[a] σ/X = ratio of standard deviation of transitions to the number of transitions/bond (both from slopes of Figs. 2–5.

decrease as temperature increases and therefore is in qualitative agreement with observation. Adopting a value of $\langle(E^* - E_0^*) >^{1/2} = 1.4$ kJ/mol that reproduces the observed value at 180 K gives rise to the results in Table 2. There it may be seen that the Gaussian result in Eq. (9) somewhat underestimates the observed trend with temperature. The question of whether this is due to an inadequacy of the Gaussian distribution in mimicking the actual one or due to some other effect is uncertain.

Acknowledgements

It is a pleasure to dedicate this contribution in honor of Wayne Mattice who has been a pioneer in the study of polymer conformation, including chain dynamics in bulk polymers. We are also indebted to the Polymers Program of the National Science Foundation for support of this work.

References

[1] McCrum NG, Read BE, Williams G. Anelastic and dielectric effects in polymeric solids. New York: Wiley, 1967.
[2] Boyd RH. Polymer 1985;26:323.
[3] Boyd RH. Polymer 1985;26:1123.
[4] Schatzki TF. J Polym Sci 1962;57:496.
[5] Boyer RF. Rubber Chem Technol 1963;34:1303.
[6] Helfand E, Wasserman ZR, Weber T. Macromolecules 1980;13:526.
[7] Adolf DB, Ediger MD. Macromolecules 1991;24:5834.
[8] Rigby D, Roe RJ. In: Roe RJ, editor. Computer simulation of polymers. Englewood Cliffs, NJ: Prentice Hall, 1991. Chapter 6.
[9] Boyd RH, Gee RH, Han J, Jin Y. J Chem Phys 1993;99:597.
[10] Jin Y, Boyd RH. J Chem Phys 1998;108:9912.
[11] Kim E-G, Mattice WL. J Chem Phys 1994;101:6242.
[12] Gee RH, Boyd RH. J Chem Phys 1994;101:8028.
[13] Pant PVK, Han J, Smith GD, Boyd RH. J Chem Phys 1993;99:597.
[14] Bharadwaj R, Boyd RH. Macromolecules 2000;33:5897.
[15] Toxvaerd S. J Chem Phys 1990;93:4290.
[16] Allen MP, Tildesley DJ. Computer simulation of liquids. Oxford: Clarendon Press, 1987.
[17] Martyna GJ, Tuckerman ME, Klein ML. J Chem Phys 1992;97:2635.
[18] Tuckerman ME, Martyna GJ, Berne BJ. J Chem Phys 1992;97:1990.
[19] Martyna GJ, Tuckerman ME, Tobias DJ, Klein ML. Mol Phys 1996;87:1117.
[20] Gee RH, Boyd RH. Comput Theor Polym Sci 1998;8:93.
[21] Boyd RH, Phillips PJ. The science of polymer molecules. Cambridge: Cambridge University Press, 1996. p. 38.